Fish and Shellfish Immunology 86 (2019) 571–580

Contents lists available at ScienceDirect

Fish and Shellfish Immunology

journal homepage: www.elsevier.com/locate/fsi

Full length article

Molecular cloning and functional characterization of a short peptidoglycan recognition protein from triangle-shell pearl mussel (*Hyriopsis cumingii*)

Ying Huang[a], Jianlin Pan[d], Xuguang Li[d], Qian Ren[b,c,*], Zhe Zhao[a,**]

[a] College of Oceanography, Hohai University, 1 Xikang Road, Nanjing, Jiangsu, 210098, China
[b] Co-Innovation Center for Marine Bio-Industry Technology of Jiangsu Province, Lianyungang, Jiangsu, 222005, China
[c] College of Marine Science and Engineering, Nanjing Normal University, 1 Wenyuan Road, Nanjing, Jiangsu, 210023, China
[d] Freshwater Fisheries Research Institute of Jiangsu Province, Nanjing, 210017, China

ARTICLE INFO

Keywords:
Hyriopsis cumingii
Peptidoglycan recognition protein
Innate immunity
Antibacterial response

ABSTRACT

Peptidoglycan (PGN) is an important target of recognition in invertebrate innate immunity. PGN recognition proteins (PGRPs) are responsible for PGN recognition. In this study, we cloned and functionally analyzed a short PGRP (*HcPGRP2*) from the triangle-shell pearl mussel *Hyriopsis cumingii*. The full-length cDNA sequence of *HcPGRP2* gene was 1185 bp containing an open reading frame of 882 bp encoding a 293 amino acid protein. HcPGRP2 was predicted to have two SH3b domains and a conserved C-terminal PGRP domain. Quantitative real-time RT-PCR showed that *HcPGRP2* was expressed in all examined tissues and its expression was induced most significantly by *Staphylococcus aureus* and *Vibrio parahaemolyticus* in the hepatopancreas and gills. RNA interference by siRNA results revealed that *HcPGRP2* was involved in the regulation of whey acidic protein, thermomacin, and defensin expression. As a pattern-recognition receptor, recombinant HcPGRP2 (rHcPGRP2) protein can bind and agglutinate (Ca^{2+} dependent) all tested bacteria. rHcPGRP2 exhibited specific binding to PGN but not to lipopolysaccharide. Moreover, rHcPGRP2 inhibited the growth activities of *S. aureus* and *V. parahaemolyticus in vitro* and accelerated the clearance of *V. parahaemolyticus in vivo*. Overall, our results indicated that HcPGRP2 may play an important role in the antibacterial immune mechanisms of *H. cumingii*.

1. Introduction

The immune system is traditionally divided into innate and acquired components [1]. Compared with vertebrates, invertebrates rely solely on their innate immunity to protect themselves against invading pathogens they do not have a real adaptive immune system [1,2]. Innate immune responses employ several kinds of germline-encoded pattern-recognition receptors (PRRs) to recognize pathogen-associated molecular patterns (PAMPs) and initiate subsequent immune cascades to eliminate harmful invaders [3,4]. PAMPs, such as bacterial lipopolysaccharide (LPS), peptidoglycan (PGN), fungal β-1,3-glucan, and viral double-stranded RNA, are highly conserved molecular structures on the microbial surface [5]. Among these PAMPs, PGNs are the essential cell wall components of most bacteria. Most Gram-positive bacteria have lysine (Lys)-type PGN, whereas Gram-negative bacteria have diaminopimelic acid (Dap)-type PGN [6]. As an ideal target molecule for bacterial invasion detection in eukaryotic organisms, PGNs are mainly recognized by a family of PRRs named PGN recognition proteins (PGRPs) [7].

PGRP was first identified from silkworm (*Bombyx mori*) hemolymph as a 19-kDa protein with the capability to trigger prophenoloxidase cascade due to its high affinity to bacterial PGN [8]. Subsequently, other PGRP homologs have been discovered in insects, mollusks and mammals, such as the 13 PGRP genes in *Drosophila melanogaster* [9], 12 in Pacific oyster *Crassostrea gigas* [10], and 4 in humans [11]. Approximately 100 PGRP family members have been identified. On the basis of the length of peptide sequences, PGRPs are categorized into three classes, namely, short and extracellular-(PGRP-S), intermediate-(PGRP-I), and long and intercellular-(PGRP-L) types, which exhibit molecular weights (MW) of approximately 20, 40–45, and 90 kDa, respectively [9–12]. Among which PGRP-S and PGRP-L are identified in some invertebrates and vertebrates [9,10], and PGRP-I only exists in mammals [11]. Structurally, most PGRPs have one PGN binding type 2 amidase domain, which is homologous to bacteriophage and bacterial type 2 amidases and is also called a PGRP domain [13]. The PGRP domain is composed of approximately 165 amino acids and hydrolyzes

* Corresponding author. College of Marine Science and Engineering, Nanjing Normal University, 1 Wenyuan Road, Nanjing, Jiangsu, 210023, China.
** Corresponding author. College of Oceanography, Hohai University, 1 Xikang Road, Nanjing, Jiangsu, 210098, China.
E-mail addresses: renqian0402@126.com (Q. Ren), zhezhao@hhu.edu.cn (Z. Zhao).

https://doi.org/10.1016/j.fsi.2018.12.007
Received 27 September 2018; Received in revised form 28 November 2018; Accepted 4 December 2018
Available online 05 December 2018
1050-4648/ © 2018 Elsevier Ltd. All rights reserved.

Table 1
Sequences of the primers used in the study.

Primers name	Sequences (5′-3′)
HcPGRP2-F	TGTTGGTGGACATACGTTGCA
HcPGRP2-R	AATGCGGCCATGATTGGATAA
UPM	
Long	CTAATACGACTCACTATAGGGCAAGCAGTGGTATCAACGCAGAGT
Short	CTAATACGACTCACTATAGGGC
5′-CDS Primer A	T_{25}VN
SMARTerIIA oligo	AAGCAGTGGTATCAACGCAGAGTACXXXXX
3′-CDS primer A	AAGCAGTGGTATCAACGCAGAGTAC(T)30VN
HcPGRP2-RT-F	GATTGCCGAAAACTATGTG
HcPGRP2-RT-R	AGTCGCTGGAAGGTGTATT
HcWAP-RT-F	TGTAATGTTGACGGGAGTG
HcWAP-RT-R	CTGTTTTGTTTTGATGGCT
HcThe-RT-F	CACAGTTGGTGGTTCAGTAA
HcThe-RT-R	CGAATCCTTCAGTAGATGGT
HcDef-RT-F	GGTGTCGTCTATCTTGCTTC
HcDef-RT-R	AGGTTATTTGGTCATCTATTTTG
β-actin-RT-F	GTGGCTACTCCTTCACAACC
β-actin-RT-R	GAAGCTAGGCTGGAACAAGG
HcPGRP2-ex-F	GGATCCCCAGGAATTCCCATGCAGATAAGAAATATGGCG
HcPGRP2-ex-R	GATGCGGCCGCTCGAGTTACTAAGAAACAAACCGCCAGGC

X = undisclosed base in the proprietary SMARTer oligo sequence.
N = A, C, G, or T; V = A, G, or C.

the amide bond in bacterial PGN [14]. In general, PGRP-S contains a single PGRP domain, PGRP-I consists of two PGRP domains, and PGRP-L has one or two PGRP domains in the C-terminus and a varied-sized N-terminal region [15].

Invertebrate PGRPs are known to be involved in innate immune systems through several different means [16]. In *Drosophila*, PGRP-SA and PGRP-SD cooperate to activate the Toll pathway in response to Lys-type PGN and initiate the transcription of antimicrobial peptide *drosomycin* [17]. Meanwhile, PGRP-LE and PGRP-LC function as signal-transducing receptors to activate the death domain-containing immune deficiency (IMD) protein and induce antimicrobial peptides (such as *diptericins* and *attacins*) to eliminate bacteria [18,19]. PGRP-SC and PGRP-LB can modulate the immune response to bacterial infection by inhibiting the activation of the IMD pathway [20]. Overexpression of PGRP-LE and constitutively activated PGRP-LC mediate the proPO cascade [21]. Furthermore, PGRPs act as opsonins to protect against microbial pathogens, such as induction of agglutination or phagocytosis and PGN hydrolysis [22,23]. All these prominent functions of PGRPs illustrate that they are vitally important to the immune system of invertebrates.

Triangle-shell pearl mussel *Hyriopsis cumingii* is an important freshwater bivalve species that is cultured in the Chinese pearl industry. However, the working mechanism of the immune system of pearl mussel against bacteria is unclear. In the current study, a cDNA for *H. cumingii* PGRP (designated as *HcPGRP2*) was cloned, and its functions were investigated. *HcPGRP2* was expressed in all examined tissues and its expression was induced most significantly by bacteria in the hepatopancreas and gills. The regulation relationship between *HcPGRP2* and antimicrobial peptides (AMPs) was demonstrated based on RNA interference (RNAi). On the basis of the critical role of PGRPs in sensing danger signals, a recombinant HcPGRP2 (rHcPGRP2) protein was generated, and its binding activities with microorganisms and specific PAMPs were demonstrated. Subsequently, rHcPGRP2 agglutinated in Gram+ and Gram− bacteria in a Ca^{2+}-dependent manner and enhanced the clearance of *Vibrio parahaemolyticus in vivo*.

2. Materials and methods

2.1. Experimental microbes and animals

Staphylococcus aureus, *Micrococcus luteus*, *Bacillus subtilis*, *Bacillus thuringiensis*, *V. parahaemolyticus*, *Aeromonas hydrophila*, and *Escherichia coli* were stored in our laboratory. All bacteria were grown in Luria–Bertani (LB) broth at 37 °C. One hundred one-year-old pearl mussels (*H. cumingii*) were obtained from the aquaculture of Wuhu City, Anhui Province, China and were maintained in fresh lake water at 25 °C before the experiments.

2.2. Immunity challenge and tissue collection

To determine tissue expression pattern of *HcPGRP2*, hemocytes, hepatopancreas, gills, and mantles were separately collected from five healthy mussels for RNA extraction. To examine the variation of *HcPGRP2* following the stimulation with 50 μL of *S. aureus* (3×10^7 cells) and *V. parahaemolyticus* (3×10^7 cells), hepatopancreas, and gills were collected from five mussels after 0, 2, 6, 12, and 24 h challenge. Total RNA was extracted by using an RNApure High-Purity Total RNA Rapid Extraction Kit (Spin-Column; Bioteke, Beijing, China), as described by the manufacturer. All RNA samples were treated with RNase-free DNase I to ensure the absence of genomic DNA. RNA (1 μg) from different samples was reverse transcribed for quantitative real-time PCR (qRT-PCR) analysis by using a PrimeScript® 1st Strand cDNA Synthesis Kit (Takara, Japan) with Oligo-d(T) Primer.

2.3. Cloning cDNA of HcPGRP2

Total RNA (5 μg) obtained from hepatopancreas was reverse transcribed by using a Clontech SMARTer™ RACE cDNA Amplification Kit (Takara, Japan) with 5′-CDS Primer A, SMARTerIIA oligos (5′-RACE Ready cDNA), and 3′-CDS Primer A (3′-RACE-Ready cDNA). Two specific primers, namely, HcPGRP2-F and HcPGRP2-R were designed (Table 1) based on the partial PGRP sequence identified in the hepatopancreas transcriptome of *H. cumingii*, and the adaptor primers (UPM) were used for 5′ and 3′ RACE. A Clontech Advantage® 2 PCR Kit from Takara (Japan) was used for gene cloning, and the program was expressed as: 5 cycles at 94 °C for 30 s and 72 °C for 3 min, followed by 5 cycles at 94 °C for 30 s, 70 °C for 30 s, 72 °C for 3 min, and 20 cycles at 94 °C for 30 s, 68 °C for 30 s, and 72 °C for 3 min. PCR products were separated on 1% agarose gel, and desired fragments were recovered by using a DNA gel extraction kit (Shanghai Generay Biotech Co., Ltd), cloned into pEasy-T3 vector (TransGen Biotech, China), and were transformed into the competent cells of *E. coli* Trans 1-T1 cells

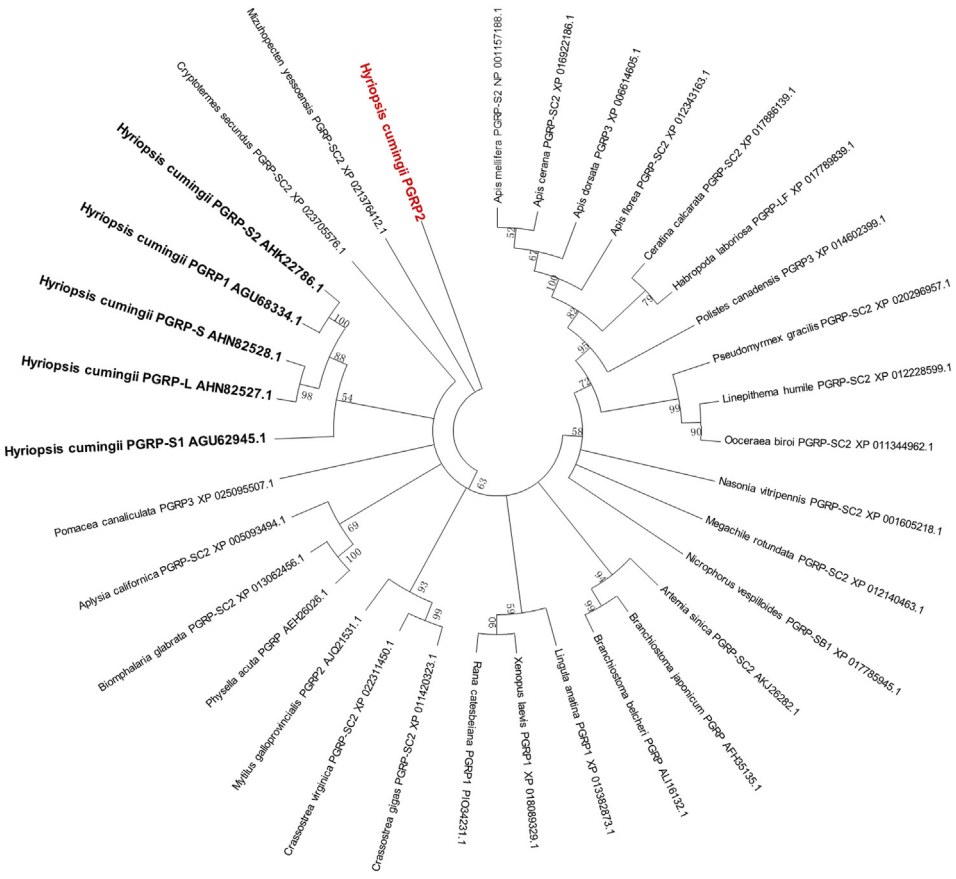

Fig. 1. Phylogenetic tree analysis of PGRP proteins. One thousand bootstraps are performed on N-J trees to evaluate the repeatability of the results in MEGA 7 software, and HcPGRP2 is marked in red. (For interpretation of the references to color in this figure legend, the reader is referred to the Web version of this article.)

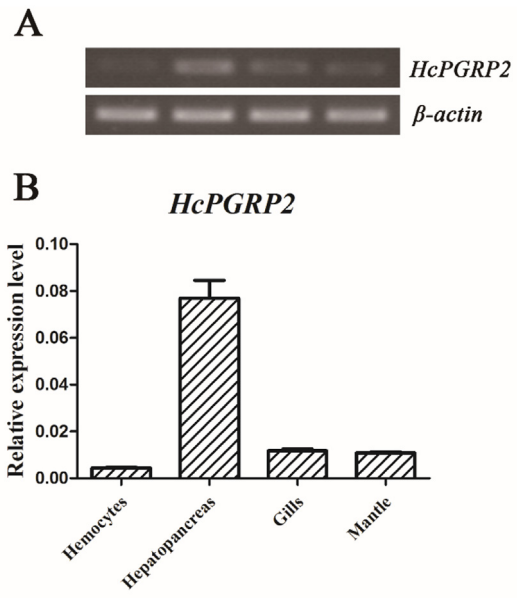

Fig. 2. Tissue transcriptional analysis of *HcPGRP2*. *HcPGRP2* expression is detected through semi-quantitative RT-PCR (A) and qRT-PCR (B) in various tissues (hemocytes, hepatopancreas, gills, and mantles) of untreated mussels. β-actin is used as a control. Each bar represents the mean value from three determinations with standard error.

(TransGen Biotech, China). The positive recombinants were identified by blue-white color selection in ampicillin-containing LB plates and were sequenced by a commercial company (Springen, China). The full length of *HcPGRP2* was obtained by overlapping EST sequences and 5′ and 3′ fragments.

2.4. Bioinformatics analysis

The cDNA sequence of *HcPGRP2* was analyzed by using the basic local alignment search tool (BLAST) algorithm from the National Center for Biotechnology Information (http://blast.ncbi.nlm.nih.gov/Blast.cgi), and the deduced protein sequences were obtained by using an Expert Protein Analysis System (ExPASy; http://web.expasy.org/). Domain organization was predicted in online software Simple Modular Architecture Research Tool (SMART; http://smart.embl-heidelberg.de/). Theoretical isoelectric point (pI) and MW were determined in ExPASy (http://web.expasy.org/compute_pi/). Further, a phylogenetic tree was constructed based on the deduced amino acid sequences by using a neighbor-joining method with 1000 bootstrap replicates in MAGA 7 software [24].

2.5. qRT-PCR analysis of HcPGRP2 expression profiles

The tissue distribution of *HcPGRP2* in the four aforementioned tissues was detected through qRT-PCR by using the primers (HcPGRP2-RT-F and HcPGRP2-RT-R) listed in Table 1. β-actin was amplified as the reference gene. qRT-PCR was performed to analyze the relative expression levels of *HcPGRP2* in the hepatopancreas and gills at different time points after *S. aureus* and *V. parahaemolyticus* challenges. qRT-PCR was conducted by using a TransStart® Top Green qPCR SuperMix Kit (TransGen Biotech, China) in LightCycler® 480 (Roche, USA). The total reaction volume was 10 μL, which contains 5 μL of 2 × TransStart Top Green qPCR SuperMix, 1 μL of 10-fold diluted cDNA, 0.2 μL (10 mM) each of forward and reverse primer, and 3.6 μL of ddH_2O. The

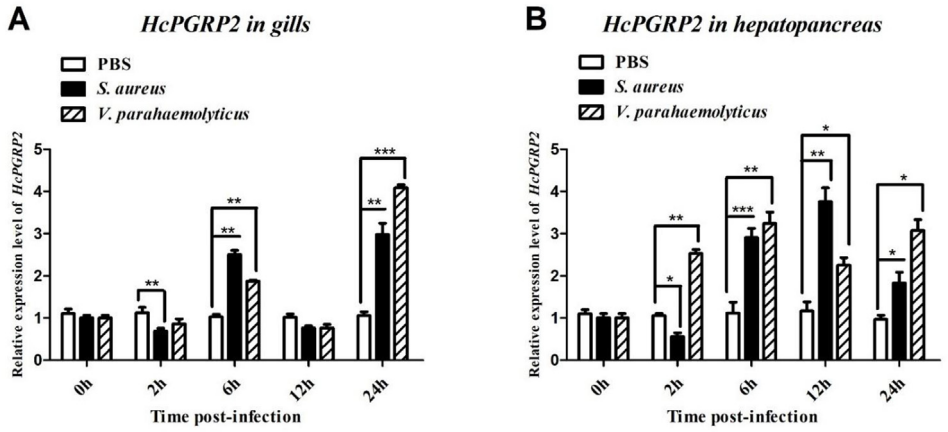

Fig. 3. Analysis of *HcPGRP2* expression in *H. cumingii* gills (A) and hepatopancreas (B) at different time points after *S. aureus* and *V. parahaemolyticus* challenges, respectively. Samples challenged with PBS are adopted as the control, and β-actin as the reference gene for internal controls. Data are shown as mean values ± standard deviations. Significance is compared between the infected and control groups at each sampling point. Asterisks indicate significant differences (*$P < 0.05$, **$P < 0.01$, ***$P < 0.001$).

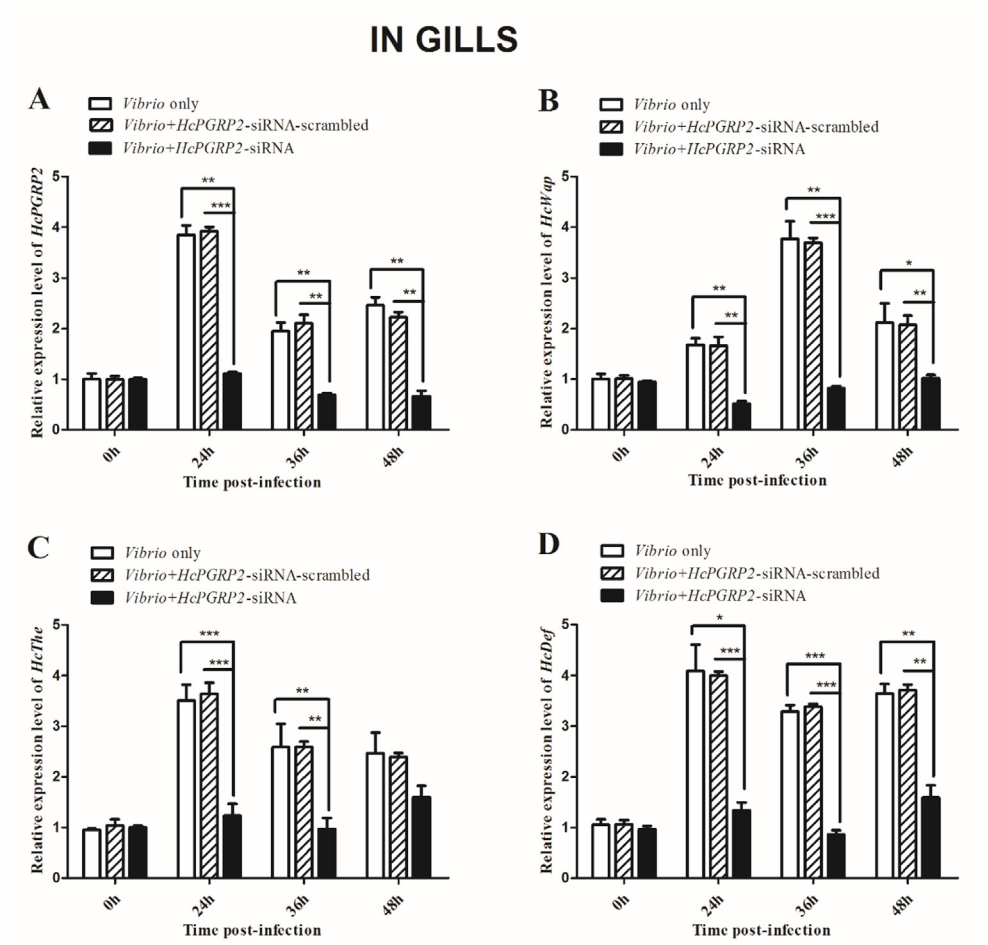

Fig. 4. *HcPGRP2* knockdown induces the changes in the expression of AMPs (*HcWAP*, *HcThe* and *HcDef*). (A) qRT-PCR analysis showing the transcription level of *HcPGRP2* in gills of *H. cumingii* after HcPGRP2-siRNA and *V. parahemolyticus* injection. The change of *HcWAP* (B), *HcThe* (C) and *HcDef* (D) at the expression level in gills at 36 h *V. parahaemolyticus* challenge (*HcPGRP2* knockdown). Random siRNA (HcPGRP2-siRNA-scrambled) is used as the control. Five mussels are selected to eliminate the individual differences at the sampled time point. Asterisks indicate significant differences (*$P < 0.05$, **$P < 0.01$, ***$P < 0.001$) compared with the values of the control.

amplification procedure included a denaturation step of 95 °C for 30 s, and 40 cycles of 95 °C for 5 s and 60 °C for 30 s, followed by a melting curve analysis from 60 °C to 95 °C. Each sample was performed in triplicate. The relative expression level of *HcPGRP2* was analyzed by using a $2^{-\Delta\Delta Ct}$ threshold cycle (C_T) method [25]. Unpaired, two-tailed *t*-test was conducted for statistical analysis, and differences less than $P < 0.05$ were considered statistically significant.

2.6. Small interfering RNA-mediated RNAi assay

On the basis of the sequence of *HcPGRP2*, a specific siRNA was synthesized based on the design rule for siRNA by using an *in vitro* transcription T7 kit according to the manufacturer's instructions (Takara, Japan). The siRNA used was *HcPGRP2*-siRNA (5′-GCACGCG GCGGATGGTTAT-3′), and this siRNA sequence was scrambled to generate the control (*HcPGRP2*-siRNA-scrambled, 5′-CGTTAGACGGTGAG CGTCG-3′). RNAi assay in mussel was conducted by injecting siRNA (30 μg/mussel) into the foot with the use of a 1-mL sterile syringe. Each mussel of the experimental (*HcPGRP2*-siRNA) and control (*HcPGRP2*-siRNA-scrambled) groups was co-injected with 15 μg of siRNA and 50 μL of *V. parahaemolyticus* (3×10^7 cells). After 12 h post-injection, 15 μg of *HcPGRP2*-siRNA or *HcPGRP2*-siRNA-scrambled was injected

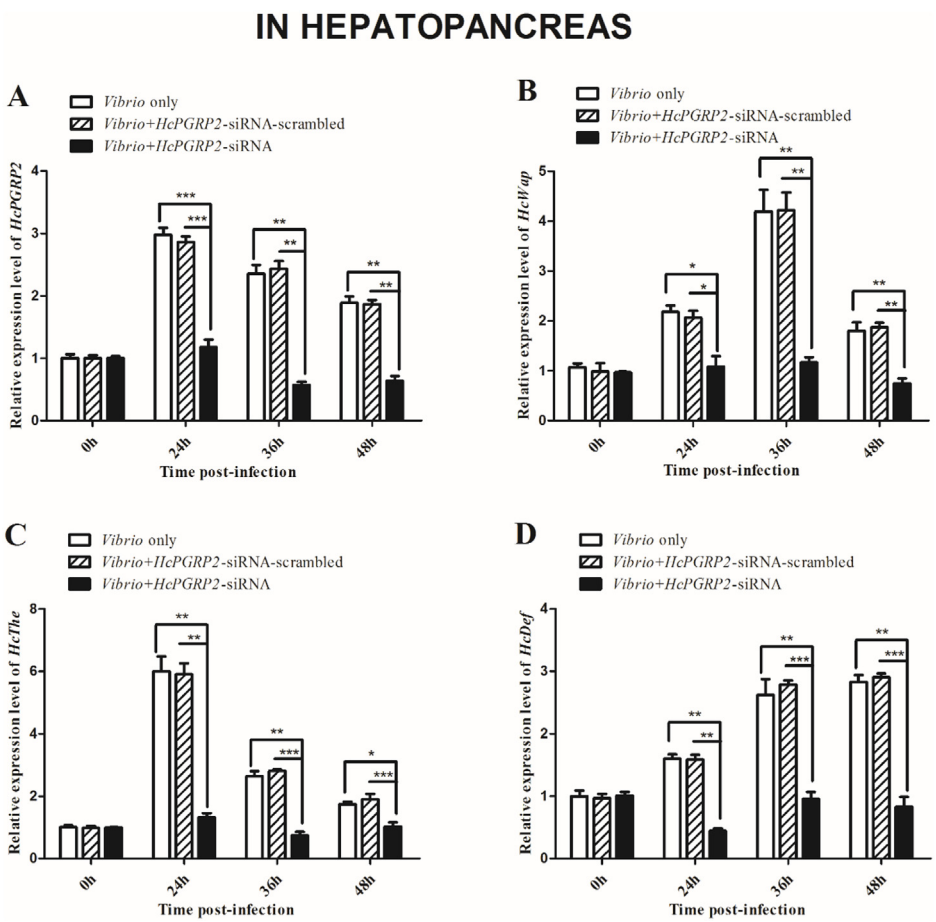

Fig. 5. *HcPGRP2* knockdown induces the changes in the expression of AMPs (*HcWAP*, *HcThe* and *HcDef*). (A) qRT-PCR analysis showing the transcription level of *HcPGRP2* in hepatopancreas of *H. cumingii* after HcPGRP2-siRNA and *V. parahemolyticus* injection. The change of *HcWAP* (B), *HcThe* (C) and *HcDef* (D) at the expression level in hepatopancreas at 36 h *V. parahaemolyticus* challenge (*HcPGRP2* knockdown). Random siRNA (HcPGRP2-siRNA-scrambled) is used as the control. Five mussels are selected to eliminate the individual differences at the sampled time point. Asterisks indicate significant differences (*$P < 0.05$, **$P < 0.01$, ***$P < 0.001$) compared with the values of the control.

into the same mussel. *V. parahaemolyticus* (3×10^7 cells) alone was injected into the mussels as control. After 24 h of the last injection, the hepatopancreas and gills of mussels in each group were separately collected for RNA extraction and cDNA synthesis. qRT-PCR was conducted to detect the efficiency of RNAi. Moreover, the mRNA expression of immune related genes was analyzed after *HcPGRP2* knockdown by using primers HcWAP-RT-F and HcWAP-RT-R, HcThe-RT-F and HcThe-RT-R, and HcDef-RT-F and HcDef-RT-R (Table 1). The assays were biologically repeated three times.

2.7. Expression and purification of recombinant HcPGRP2

cDNA fragment encoding the mature peptide of *HcPGRP2* was amplified with specific primers (HcPGRP2-ex-F and HcPGRP2-ex-R, Table 1), which contain *EcoR* I and *Xho* I sites at their 5′ ends. After digestion, the PCR product was cloned into pGEX-6p-2 vector and was transformed into *E. coli* BL21 (DE3) competent cells (TransGen Biotech, China). Positive clones were grown in 300 mL LB medium at 37 °C with shaking at 200 rpm with OD600 of 0.6. Isopropyl-β-D-thiogalactoside (IPTG) was added to the medium to obtain a final concentration of 0.5 mM to induce expression, and the cultures were incubated at 37 °C at 200 rpm for 5 h. The bacteria were pelleted through centrifugation at 6000 rpm for 10 min and were re-suspended in cold PBS containing 0.1% Triton X-100 for probe sonication lysis. The recombinant HcPGRP2 protein with an N-terminal glutathione S-transferase (GST) tag (GST-HcPGRP2) was purified through glutathione Sepharose 4B chromatography (Gen-Script, USA) following the manufacturer's instruction. The empty pGEX-6p-2 vector without any insert was transformed into BL21 (DE3) cells, and the GST-tag protein (GST) was similarly expressed and purified. GST was used as the control protein in some assays. Purified proteins were examined through 12.5% SDS-polyacrylamide gel electrophoresis (SDS-PAGE) and were visualized with Coomassie brilliant blue R250.

2.8. Microbial binding and agglutination assays

The purified rHcPGRP2 (100 μg) was incubated with seven strains of bacteria (approximately 2×10^8 cells each) comprising four Gram-positive bacteria, namely, *S. aureus*, *M. luteus*, *B. subtilis*, and *B. thuringiensis*, and three Gram-negative bacteria, namely, *V. parahaemolyticus*, *A. hydrophila*, and *E. coli*. The mixtures were subjected to gentle rotation at 37 °C for 1 h. Subsequently, the microorganisms were pelleted, centrifuged at 6000 rpm for 5 min, washed four times with TBS (20 mM Tris-HCl, 150 mM NaCl, pH 7.4), and were analyzed by Western blotting with anti-GST rabbit antibody. Bacterial cells cultured with GST-tag protein were used as controls.

Bacterial agglutination assay was performed, as previously reported [26]. Briefly, *S. aureus* and *V. parahaemolyticus* were cultured in LB medium at 37 °C to an OD600 of 0.8. The cells were harvested by centrifugation at 6000 rpm for 5 min and were re-suspended in TBS buffer. In the presence or absence of 10 mM $CaCl_2$, 25 μL of rHcPGRP2 (100 μg/mL) was mixed with 25 μL of bacteria suspension. GST (100 μg/mL) or bovine serum albumin (BSA) (100 μg/mL) was mixed with bacterial cells and was used as the negative control. The mixtures were incubated at room temperature for 1 h. Agglutinating reactions were observed through microscopy (Nikon, Japan).

2.9. PAMP binding assay

The PAMP binding activity of rHcPGRP2 was examined through enzyme-linked immunosorbent assay (ELISA), as previously described [26]. In particular, LPS and PGN were dissolved in distilled water with

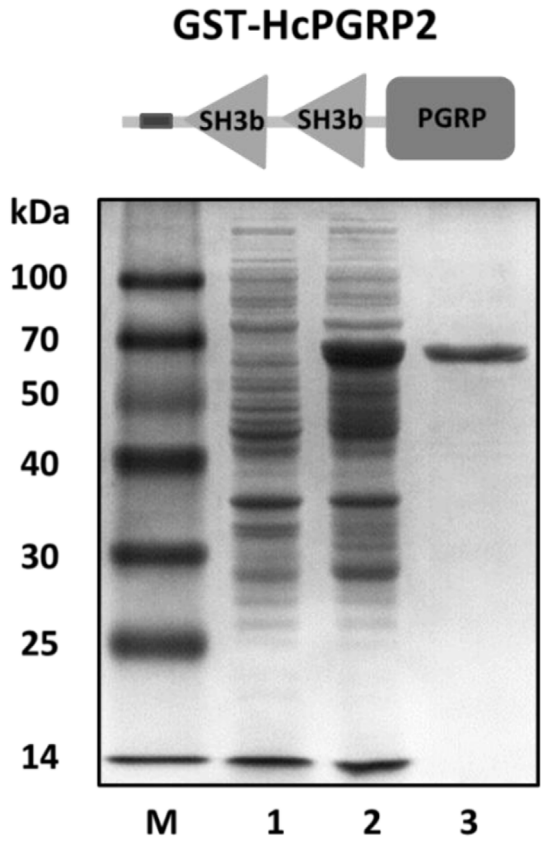

Fig. 6. Recombinant expression and purification of HcPGRP2 (Lane M: standard protein marker; Lane 1: crude protein extracts of *E. coli* without induction; Lane 2: crude protein extracts of *E. coli* after induction for 5 h by IPTG; and Lane 3: purified recombinant protein).

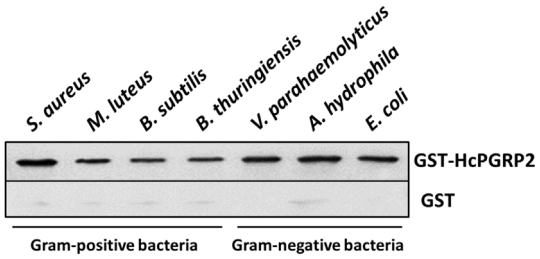

Fig. 7. Direct binding of rHcPGRP2 to various bacteria. Binding activities of rHcPGRP2 against G+ bacteria (*S. aureus*, *M. luteus*, *B. subtilis*, and *B. thuringiensis*) and G− bacteria (*V. parahaemolyticus*, *A. hydrophila*, and *E. coli*) are investigated through Western blot analysis.

80 μg/mL concentration and were sonicated for 3 s × 15 s on ice. Polysaccharides (4 μg) (50 μL) were coated to each well of 96-well plates, incubated at 37 °C overnight, heated at 60 °C for 30 min, and were blocked with 3% BSA in TBS (200 μL/well) at 37 °C for 2 h. The purified rHcPGRP2 was diluted in TBS under different concentrations of 0.78, 1.56, 3.125, 6.25, 12.5, and 25 μg/mL. The plates were incubated with the recombinant protein at room temperature for 3 h, washed with TBS four times, and were incubated with rabbit monoclonal anti-GST antibody (1: 2000 dilution in TBS with 0.1 mg/mL BSA) for 2 h at 37 °C. The plates were washed again and incubated with peroxidase-conjugated goat anti-rabbit IgG secondary antibodies (1: 5000 dilution in TBS with 0.1 mg/mL BSA) at 37 °C for 1 h. After the last wash, color was developed with 100 μL of 0.01% 3, 3′, 5, 5′-tetramethylbenzidine (Sigma), and the reaction was stopped by adding 2 M H_2SO_4. The absorbance at 450 nm for each well was read by using a plate reader (BioTek Instruments, USA). All assays were repeated thrice.

2.10. Antibacterial activity and V. parahaemolyticus clearance assay

The effect of rHcPGRP2 on the growth curves of *S. aureus* and *V. parahaemolyticus* was investigated, as described in our previous report [27]. Single colony was transferred into 5 mL of LB broth, rHcPGRP2 was added at the finial concentration of 100 μg/mL, and purified GST-tag protein was used as the negative control. Each sample was incubated at 37 °C with shaking at 200 rpm, and OD450 was measured every 1 h.

Bacterial clearance assay was performed to investigate the involvement of rHcPGRP2 in *V. parahaemolyticus* clearance. Purified rHcPGRP2 (100 μg/mL, 500 μL) was incubated with *V. parahaemolyticus* (2×10^8 cells, 500 μL) at 37 °C for 1 h with gentle rotation. GST (100 μg/mL, 500 μL) was incubated with the same number of *V. parahaemolyticus* as the control group. After incubation, 50 μL of the mixture was injected into the mussels. Hemolymph was collected by using a 1 mL syringe preloaded with 500 μL of anticoagulant buffer at 2, 10, and 20 min. The serial diluted hemolymph was plated on LB plates. After the incubation of plates at 37 °C overnight, the number of single bacterial clones was counted, and the number of bacteria per milliliter of hemolymph was calculated.

3. Result

3.1. Characterization of HcPGRP2 cDNA

The full-length cDNA sequence of *HcPGRP2* gene from freshwater pearl mussel *H. cumingii* was 1185 bp in length, which contains a 5′-untranslated region (UTR) of 1 bp, an open reading frame of 882 bp encoding a 293 amino acid protein, and a 303 bp 3′-UTR with a predicted alternative polyadenylation signal site (AATAAA) and a poly(A) tail (Fig. S1). HcPGRP2 was predicted to have two SH3b (src Homology-3) domains (amino acids 25–93 and 103–171) and a conserved C-terminal PGRP domain (amino acids 193–293), but lacked a typical signal peptide. The HcPGRP2 protein was estimated to have an MW of 32564.28 Da with PI of 8.17.

3.2. Phylogenetic analysis

Sequence analysis with the BLASTX algorithm showed that the deduced amino acid sequence of HcPGRP2 displays the highest identity of 73% to *Mytilus galloprovincialis* PGRP2 (AJQ21531.1), 66% identities with *Lingula anatina* PGRP1 (XP_013382873.1), 65% identities with *C. gigas* PGRP-SC2 (EKC26200.1), and 64% identities with *Crassostrea virginica* PGRP-SC2 (XP_022289441.1). The multiple alignments of HcPGRP2, HcPGRP1 (AGU68334.1), HcPGRP-L (AHN82527.1), HcPGRP-S (AHN82528.1), HcPGRP-S1 (AGU62945.1), and HcPGRP-S2 (AHK22786.1) showed the diversity of amino acid sequences (Fig. S2), and the key amino acids within PGRP domains were conserved. Moreover, a phylogenetic tree based on the amino acid sequences of HcPGRP2 and homologs was constructed to reveal the evolutional relationships (Fig. 1). All *H. cumingii* PGRPs were clustered into the same group, and the HcPGRP2 in the present study formed an independent branch that was isolated from all of invertebrate PGRPs.

3.3. Tissue distribution and expression analysis of HcPGRP2

Tissue level expression of *HcPGRP2* mRNA was analyzed through RT-PCR and qRT-PCR by using β-actin as a control. *HcPGRP2* expression was detected in various tissues, such as hemocytes, hepatopancreas, gills, and mantles. *HcPGRP2* expression was mainly detected in hepatopancreas and a few levels in gills, mantles, and hemocytes (Fig. 2A and B).

The temporal expression pattern of *HcPGRP2* post-bacterial challenge was determined through qRT-PCR. Results revealed that the transcription of *HcPGRP2* was significantly upregulated ($P < 0.01$) in

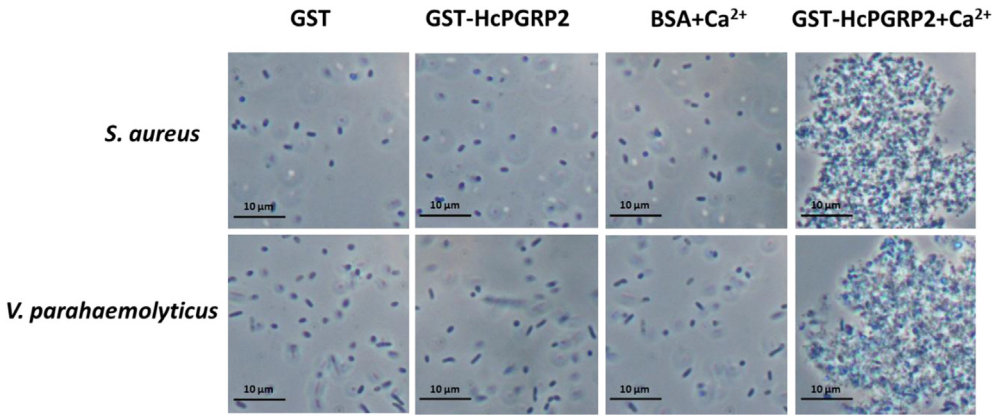

Fig. 8. Microorganism agglutination activity of rHcPGRP2. The agglutination activity of rHcPGRP2 is evaluated against G+ bacteria *S. aureus* and G− *V. parahaemolyticus* in the presence of 10 mM $CaCl_2$. GST-tag protein and BSA are used as positive and negative controls, respectively.

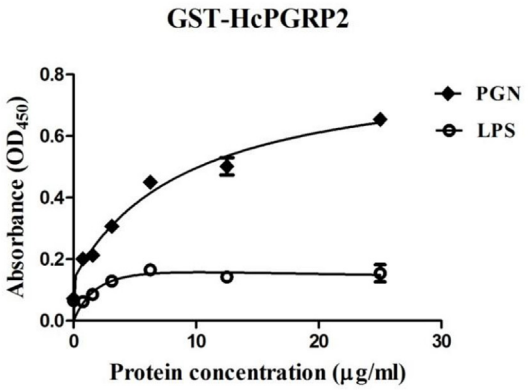

Fig. 9. Binding of rHcPGRP2 to polysaccharides determined through ELISA *in vitro*. ELISA is used to quantify the binding of purified rHcPGRP2 to LPS and PGN. The data are the average ± SD of three independent cultures.

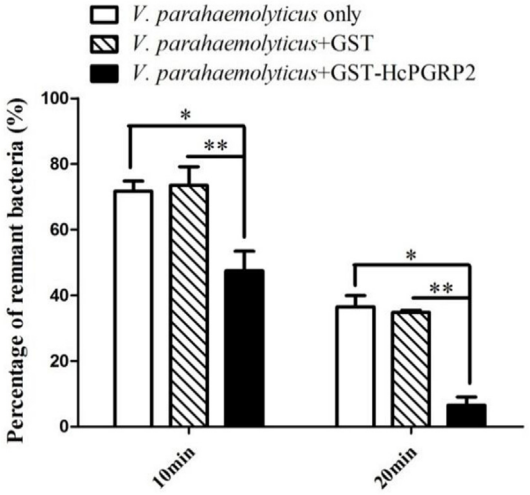

Fig. 11. *In vivo* bacterial clearance activity of rHcPGRP2. Mussels are injected with *V. parahaemolyticus* pre-incubated with rHcPGRP2 or GST. The number of remaining bacteria is counted at 2, 10, and 20 min post-injection. The percentage of remnant bacteria is calculated (percentage of remnant bacteria = No. of bacteria at 10 min or 20 min/No. of bacteria at 2 min × 100%). Error bars represent ± SD of three replicates. Asterisks indicate significant differences (*$P < 0.05$, **$P < 0.01$) compared with the values of the control.

gills at 6 h and 24 h post *S. aureus* and *V. parahaemolyticus* challenge, which reach up to 2.5 and 3 times and 1.8 and 4 times, respectively (Fig. 3A). In hepatopancreas, the expression levels of *HcPGRP2* reached the maximum at 12 h or 6 h with 3.7-fold or 3.2-fold compared with those in the controls after *S. aureus* and *V. parahaemolyticus* challenges, respectively (Fig. 3B). No remarkable variation in expression was observed in the control samples induced by PBS.

3.4. Effect of HcPGRP2 silencing on immune-related genes

RNAi assay was conducted to investigate *HcPGRP2* function in *H.*

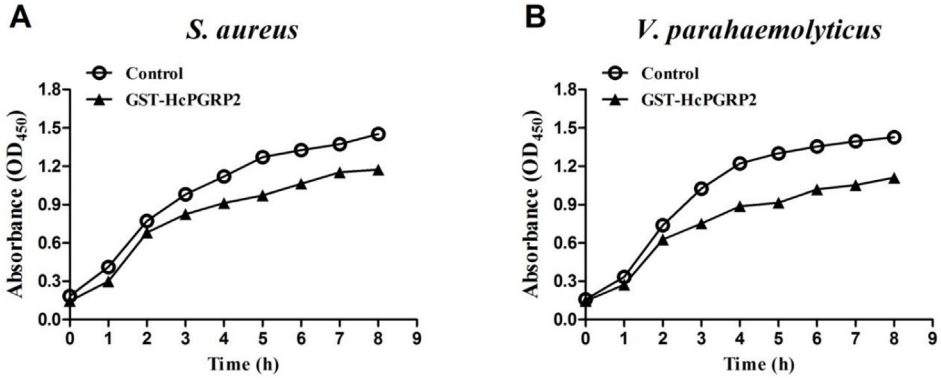

Fig. 10. Bacterial growth inhibition by rHcPGRP2. The growth inhibition of cultured *S. aureus* (A) and *V. parahaemolyticus* (B) is examined by using rHcPGRP2 with final concentration of 100 μg/mL. After incubation at 37 °C, the bacterial culture is taken every 1 h to measure the absorbance at 450 nm.

cumingii. The efficiency of HcPGRP2-siRNA was assessed through qRT-PCR. Compared with those in *V. parahaemolyticus* only group or HcPGRP2-siRNA-scrambled group, the mRNA levels of *HcPGRP2* in the gills and hepatopancreas were extremely downregulated at 36 h after HcPGRP2-siRNA and *V. parahaemolyticus* injection, and no suppression was observed on *HcPGRP2* in the random siRNA and *V. parahaemolyticus* groups (Figs. 4A and 5A). These results indicated that HcPGRP2 siRNA can remarkably inhibit the expression of *HcPGRP2* gene in *H. cumingii*. The expression levels of three AMPs in the gills and hepatopancreas under the same condition were investigated based on these results. Time course expression profiles of whey acidic protein (*HcWAP*), theromacin (*HcThe*), and defensin (*HcDef*) were detected through qRT-PCR. As shown in Fig. 4B–D and 5B–D, the transcription of the three AMPs can be induced by *V. parahemolyticus* and can be suppressed by *HcPGRP2* knockdown.

3.5. Expression and purification of recombinant HcPGRP2

The recombinant plasmid pGEX-6p-2-HcPGRP2 was transformed and expressed in BL21 (DE3) cells. After IPTG induction, the total cell lysate was analyzed through SDS-PAGE, and a distinct band was observed (approximately 59 kDa), which was in accordance with the putative molecular mass of rHcPGRP2 (predicted MW of 33 kDa plus a GST-tag protein 26 kDa) (Fig. 6, lane 2). rHcPGRP2 was successfully purified after purification of glutathione Sepharose 4B chromatography (Fig. 6, lane 3).

3.6. Microbial binding and agglutination of rHcPGRP2

PRRs initiate multiple immune responses against pathogens after PAMP recognition. Microorganism binding and agglutination assays were conducted to investigate the interaction between rHcPGRP2 and pathogens. Bacterial binding assay showed that rHcPGRP2 can bind to all tested G+ bacteria (*S. aureus*, *M. luteus*, *B. subtilis*, and *B. thuringiensis*) and G− bacteria (*V. parahaemolyticus*, *A. hydrophila*, and *E. coli*) (Fig. 7). In the presence of calcium (10 mM), rHcPGRP2 had the capability to agglutinate *S. aureus* (G+) and *V. parahaemolyticus* (G−) compared with GST or BSA (Fig. 8). Thus, rHcPGRP2 agglutinated the bacteria, and the agglutinating activity of rHcPGRP2 was Ca^{2+}-dependent.

3.7. PAMP binding of rHcPGRP2

Direct binding to polysaccharides was determined through ELISA to investigate the binding specificity of rHcPGRP2 to sugars. Purified rHcPGRP2 can bind to PGN in a dose-dependent manner (Fig. 9). However, rHcPGRP2 was unable to directly bind LPS *in vitro* (Fig. 9). GST and BSA controls failed to show PAMP binding, as expected (data not shown).

3.8. Bacterial growth inhibition and V. parahaemolyticus clearance assay

The inhibitory effect of rHcPGRP2 on the growth curves of *S. aureus* (Fig. 10A) and *V. parahaemolyticus* (Fig. 10B) was evaluated, and rHcPGRP2 (100 μg/mL) strongly suppressed the growth of the two bacteria compared with the control groups. The bacteria had slow growth without obvious difference in all the experimental groups at 0–2 h, and rHcPGRP2 significantly suppressed microbial growth at 3–8 h (logarithmic phase). The clearance activity of rHcPGRP2 toward *V. parahaemolyticus* was evaluated by inoculation of mussel with the bacterium pre-incubated with rHcPGRP2. GST was used as a control. As shown in Fig. 11, the clearance of *V. parahaemolyticus* in rHcPGRP2 treatment, which is recorded as the percentage of residual cells in hemolymph, was promoted with a higher rate than that of the control groups.

4. Discussion

In the present work, a new PGRP (*HcPGRP2*) in freshwater pearl mussel *H. cumingii* was cloned and functionally analyzed. The predicted HcPGRP2 protein and the previously reported HcPGRP-S1 [29], HcPGRP1, and HcPGRP1a [30] belonged to the PGRP gene family of *H. cumingii*. HcPGRP2 was approximately 33 kDa with two SH3b domains and one typical PGRP domain. In fact, PGRP with two SH3b domains was rare. SH3 domain homologs have been found in bacterial proteins, and they may mediate many diverse processes, such as increasing the local concentration of proteins and altering their subcellular location [31]. These structural features revealed that HcPGRP2 may have bacterial recognition and effector functions to eliminate pathogens.

The transcript of *HcPGRP2* gene was detected in all of the examined tissues with the highest expression in hepatopancreas, which is similar to other PGRPs in *H. cumingi* [29,30]. On the basis of existing reports, Mollusk PGRPs have shown highly variable expression in various tissues. The mRNA of *AiPGRP* was highly expressed in hemocytes of bay scallop *Argopecten irradians* [32], and *CgPGRP-S1L* and *CgPGRP-S3* transcripts were mainly present in mantles and digestive diverticula of oyster *C. gigas*, respectively [33]. *Solen grandis* SgPGRP-S1 was predominantly expressed in hepatopancreas, gonad, and intestinal [34]. Various PGRPs were selectively expressed in different organs, which suggest that they may display distinct physiological functions. The high expression of *HcPGRP2* in hepatopancreas suggested its involvement in innate immunity. After exposure to bacteria, the expression patterns of PGRPs considerably varied among the host species. Three PGRPs from *H. cumingi* in different tissues (*HcPGRP-S1* in gonad, nephridium, gill and foot [29]; *HcPGRP1* in hepatopancreas and foot [30]; *HcPGRP1a* in hepatopancreas, foot and gills [30]) were significantly induced in response to LPS or PGN challenge. Stimulation with *Marinococcus halophilus* and *Vibrio tubiashii* significantly upregulated the temporal expression of *CgPGRP-L* from *C. gigas*, which indicates that this inducible protein is involved in the immune response to invading microbes [35]. Similarly, *CfPGRP-S1* in hemocytes from *Chlamys farreri* markedly induced in response to challenge of *Micrococcus lysodeikticus* or *Vibrio anguillarum* [36]. In this study, *S. aureus* and *V. parahaemolyticus* induced the expression of *HcPGRP2* in hepatopancreas and gills, which indicate the importance of *HcPGRP2* as innate PRRs in immune defense.

The primary function of PGRPs is PGN recognition and binding. The interactions of HcPGRP2 with microbial polysaccharides (LPS and PGN) were investigated to elucidate whether HcPGRP2 had the similar function. ELISA experiments demonstrated that rHcPGRP2 protein exhibits specific binding to PGN, and no activity was observed in LPS. Consistent with this finding, rHcPGRP-S1 from *H. cumingi* [29] and rSgPGRP-S1 from *S. grandis* [37] were able to bind Lys-type and DAP-type PGNs, whereas rCgPGRP-S1S bound to DAP-type PGN, but not to Lys-type PGN [38]. Moreover, rHcPGRP2 bound to G+ and G− bacteria with varying binding affinities to different kinds of bacteria, whereas rCgPGRP-S1S had a high affinity to *E. coli*, but not to the other tested DAP-type PGN bacteria, *V. anguillarum* and *B. subtilis*, when living bacteria were used in binding assays [38]. PGRPs recognize and bind bacteria through PGN on their cell wall [7]. The contradiction between PGN and living bacteria in bumblebee *Bombus ignitus* BiPGRP-S was reported [39]. The recognition of some PGRPs may depend on the primary PGN structures and may be influenced by other factors [40].

On the basis of the binding activity to *S. aureus* and *V. parahaemolyticus* cells, HcPGRP2 was considered a key factor to control *S. aureus* and *V. parahaemolyticus* invasion. As a direct influence of HcPGRP2 on the two bacteria, agglutination was observed in the presence of rHcPGRP2 and calcium. Similar bacterial agglutination properties were reported for three bivalve PGRPs, SgPGRP-S1 from *S. grandis* [37], CfPGRP-S1 from *Zhikong scallop* [41], and CgPGRP-S1S from *C. gigas* [38]. Generally, bacterial agglutination plays a role in infection control by concentrating pathogens or preventing their propagation in the host [42]. Another notable immune behavior mediated by PGRPs is

the antibacterial response. This study revealed that rHcPGRP2 inhibits the growth of *S. aureus* and *V. parahaemolyticus in vitro*. Similarly, rSgPGRP-S1 exhibited obvious bactericidal activity against Gram-positive *S. aureus* and Gram-negative *E. coli* [37]. Moreover, *V. parahaemolyticus* clearance assay demonstrated its inhibition *in vivo*. *V. parahaemolyticus* is an important pathogen to invertebrate and vertebrate organisms and can induce immune response in mussels [43]. rHcPGRP2 facilitated the clearance of *V. parahaemolyticus*, which is similar with SgPGRP-S1 [37] and CfPGRP-S1 [41]. In *Drosophila*, Gram + and Gram − bacteria are recognized by different PGRPs, and distinct signaling pathways are initiated to eliminate non-self invasions [7,9]. PGRPs can trigger the activation of downstream Toll, IMD, JNK, and proPO signaling pathways [18,19,21]. The present data suggested that rHcPGRP2 is involved in the immune response of *H. cumingii* under *V. parahaemolyticus* challenge, which is related to the regulation of antimicrobial peptides (*HcWAP*, *HcThe* and *HcDef*) expression. Therefore, HcPGRP2 plays an important role in the antibacterial immune mechanisms of freshwater pearl mussels.

In summary, a PGRP gene (HcPGRP2) was successfully cloned from *H. cumingii*. HcPGRP2 was constitutively expressed in the tissues of normal mussels. Functional analysis revealed that HcPGRP2 has multi-immune activities, such as PGN binding, microorganism binding, agglutination, antibacterial activity, and immune gene regulation. Our findings will provide some references for future investigations on antimicrobial immunity in *H. cumingii*.

Author contributions

Y.H. and Q.R. carried out the experiments. Y.H. J.L.P. X.G.L and Q.R. designed the experiments and analyzed the data. Y.H. Q.R. and Z.Z. contributed reagents/materials. Y.H. Q.R. and Z.Z. wrote the manuscript. All authors gave final approval for publication.

Disclosure of potential conflicts of interest

No potential conflicts of interest were disclosed.

Acknowledgments and funding

The current study was supported by the Fundamental Research Funds for the Central Universities (2018B03214), the Natural Science Foundation of Jiangsu Province (BK20180501, BK20171474, BK20161602), the National Natural Science Foundation of China (Grant No. 31572647), the Natural Science Fund of Colleges and universities in Jiangsu Province (14KJA240002), the Science and Technology Planning Project of Jiangsu Province (BE2017383), the Jiangsu Fisheries Research System (JFRS-05), and the Project Funded by the Priority Academic Program Development of Jiangsu Higher Education Institutions (PAPD).

Appendix A. Supplementary data

Supplementary data to this article can be found online at https://doi.org/10.1016/j.fsi.2018.12.007.

References

[1] B. Beutler, Innate immunity: an overview, Mol. Immunol. 40 (2004) 845–859.
[2] E.S. Loker, C.M. Adema, S.M. Zhang, T.B. Kepler, Invertebrate immune systems–not homogeneous, not simple, not well understood, Immunol. Rev. 198 (2004) 10–24.
[3] C.A. Janeway Jr., R. Medzhitov, Innate immune recognition, Annu. Rev. Immunol. 20 (2002) 197–216.
[4] R. Medzhitov, C.A. Janeway Jr., Decoding the patterns of self and nonself by the innate immune system, Science 296 (2002) 298–300.
[5] R. Medzhitov, C.A. Janeway Jr., Innate immune recognition: mechanisms and pathways, Immunol. Rev. 173 (2000) 89–97.
[6] W. Vollmer, D. Blanot, M.A. de Pedro, Peptidoglycan structure and architecture, FEMS (Fed. Eur. Microbiol. Soc.) Microbiol. Rev. 32 (2008) 149–167.
[7] S. Kurata, Peptidoglycan recognition proteins in Drosophila immunity, Dev. Comp. Immunol. 42 (2014) 36–41.
[8] H. Yoshida, K. Kinoshita, M. Ashida, Purification of peptidoglycan recognition protein from hemolymph of the silkworm, *Bombyx mori*, J. Biol. Chem. 271 (1996) 13854–13860.
[9] T. Werner, G. Liu, D. Kang, S. Ekengren, H. Steiner, D. Hultmark, A family of peptidoglycan recognition proteins in the fruit fly *Drosophila melanogaster*, Proc. Natl. Acad. Sci. U. S. A 97 (2000) 13772–13777.
[10] Y. Zhang, Z. Yu, The first evidence of positive selection in peptidoglycan recognition protein (PGRP) genes of *Crassostrea gigas*, Fish Shellfish Immunol. 34 (2013) 1352–1355.
[11] C. Liu, Z. Xu, D. Gupta, R. Dziarski, Peptidoglycan recognition proteins: a novel family of four human innate immunity pattern recognition molecules, J. Biol. Chem. 276 (2001) 34686–34694.
[12] G. Coteur, P. Mellroth, C. De Lefortery, D. Gillan, P. Dubois, D. Communi, Peptidoglycan recognition proteins with amidase activity in early deuterostomes (Echinodermata), Dev. Comp. Immunol. 31 (2007) 790–804.
[13] R. Dziarski, Peptidoglycan recognition proteins (PGRPs), Mol. Immunol. 40 (2004) 877–886.
[14] J. Royet, D. Gupta, R. Dziarski, Peptidoglycan recognition proteins: modulators of the microbiome and inflammation, Nat. Rev. Immunol. 11 (2011) 837–851.
[15] Q.L. Sun, L. Sun, A short-type peptidoglycan recognition protein from tongue sole (*Cynoglossus semilaevis*) promotes phagocytosis and defense against bacterial infection, Fish Shellfish Immunol. 47 (2015) 313–320.
[16] R. Dziarski, D. Gupta, The peptidoglycan recognition proteins (PGRPs), Genome Biol. 7 (2006) 232.
[17] T. Michel, J.M. Reichhart, J.A. Hoffmann, J. Royet, *Drosophila* Toll is activated by gram-positive bacteria through a circulating peptidoglycan recognition protein, Nature 414 (2001) 756–759.
[18] T. Tanji, Y.T. Ip, Regulators of the Toll and Imd pathways in the *Drosophila* innate immune response, Trends Immunol. 26 (2005) 193–198.
[19] T. Tanji, X. Hu, A.N. Weber, Y.T. Ip, Toll and IMD pathways synergistically activate an innate immune response in *Drosophila melanogaster*, Mol. Cell Biol. 27 (2007) 4578–4588.
[20] J.C. Paredes, D.P. Welchman, M. Poidevin, B. Lemaitre, Negative regulaiton by amidase PGRPs shapes the *Drosophila* antibacterial response and protects the fly from innocuous infection, Immunity 35 (2011) 770–779.
[21] F. Maillet, V. Bischoff, C. Vignal, J. Hoffmann, J. Royet, The *Drosophila* peptidoglycan recognition protein PGRP-LF blocks PGRP-LC and IMD/JNK pathway activation, Cell Host Microbe 3 (2008) 293–303.
[22] P. Mellroth, J. Karlsson, H. Steiner, A scavenger function for a *Drosophila* peptidoglycan recognition protein, J. Biol. Chem. 278 (2003) 7059–7064.
[23] C.I. Chang, S. Pili-Floury, M. Hervé, C. Parquet, Y. Chelliah, B. Lemaitre, D. Mengin Lecreulx, J. Deisenhofer, A *Drosophila* pattern recognition receptor contains a peptidoglycan docking groove and unusual L,D-carboxypeptidase activity, PLoS Biol. 2 (2004) E277.
[24] S. Kumar, G. Stecher, K. Tamura, MEGA7: molecular evolutionary Genetics analysis version 7.0 for bigger datasets, Mol. Biol. Evol. 33 (2016) 1870–1874.
[25] K.J. Livak, T.D. Schmittgen, Analysis of relative gene expression data using real-time quantitative PCR and the 2 (–ΔΔC(T)) method, Methods 25 (2001) 402–408.
[26] Y. Huang, L. An, K.M. Hui, Q. Ren, W. Wang, An LDLa domain-containing C-type lectin is involved in the innate immunity of *Eriocheir sinensis*, Dev. Comp. Immunol. 42 (2013) 333–344.
[27] Y. Huang, W. Wang, Q. Ren, Function of gC1qR in innate immunity of Chinese mitten crab, *Eriocheir sinensis*, Dev. Comp. Immunol. 61 (2016) 34–41.
[29] Z. Yang, J. Li, Y. Li, H. Wu, X. Wang, Molecular cloning and functional characterization of a short peptidoglycan recognition protein (HcPGRPS1) from the freshwater mussel, *Hyriopsis cumingi*, Mol. Immunol. 56 (2013) 729–738.
[30] Y. Tao, Z.Y. Yang, X. Zhang, H.J. Wu, Molecular cloning and mRNA expression of the peptidoglycan recognition protein gene HcPGRP1 and its isoform HcPGRP1a from the freshwater mussel *Hyriopsis cumingi*, Genet. Mol. Biol. 37 (2014) 508–517.
[31] N. Ringstad, Y. Nemoto, P. De Camilli, The SH3p4/Sh3p8/SH3p13 protein family: binding partners for synaptojanin and dynamin via a Grb2-like Src homology 3 domain, Proc. Natl. Acad. Sci. U. S. A 94 (1997) 8569–8574.
[32] D. Ni, L. Song, L. Wu, L.T. Wu, Y.Q. Chang, Y.D. Yu, Molecular cloning and mRNA expression of peptidoglycan recognition protein (PGRP) gene in bay scallop (*Argopecten irradians*, Lamarck 1819), Dev. Comp. Immunol. 31 (2007) 548–558.
[33] N. Itoh, K.G. Takahashi, Distribution of multiple peptidoglycan recognition proteins in the tissues of Pacific oyster, *Crassostrea gigas*, Comp. Biochem. Physiol. B Biochem. Mol. Biol. 150 (2008) 409–417.
[34] X.M. Wei, J.M. Yang, D.L. Yang, J. Xu, X.Q. Liu, J.L. Yang, Molecular cloning and mRNA expression of two peptidoglycan recognition protein (PGRP) genes from mollusk *Solen grandis*, Fish Shellfish Immunol. 32 (2012) 178–185.
[35] N. Itoh, K.G. Takahashi, A novel peptidoglycan recognition protein containing a goose-type lysozyme domain from the Pacific oyster, *Crassostrea gigas*, Mol. Immunol. 46 (2009) 1768–1774.
[36] J.G. Su, D.J. Ni, L.S. Song, J.M. Zhao, L.M. Qiu, Molecular cloning and characterization of a short type peptidoglycan recognition protein (CfPGRP-S1) cDNA from Zhikong scallop *Chlamys farreri*, Fish Shellfish Immunol. 23 (2007) 646–656.
[37] X. Wei, D. Yang, H. Li, T. Zhao, H. Jiang, X. Liu, J. Yang, Peptidoglycan recognition protein of *Solen grandis* (SgPGRP-S1) mediates immune recognition and bacteria clearance, Fish Shellfish Immunol. 73 (2018) 30–36.
[38] M. Iizuka, T. Nagasaki, K.G. Takahashi, M. Osada, N. Itoh, Involvement of *Pacific oyster* CgPGRP-S1S in bacterial recognition, agglutination and granulocyte degranulation, Dev. Comp. Immunol. 43 (2014) 30–34.
[39] H. You, H. Wan, J. Li, B.R. Jin, Molecular cloning and characterization of a short

peptidoglycan recognition protein (PGRP-S) with antibacterial activity from the bumblebee *Bombus ignites*, Dev. Comp. Immunol. 34 (2010) 977–985.
[40] K.H. Schleifer, O. Kandler, Peptidoglycan types of bacterial cell walls and their taxonomic implications, Bacteriol. Rev. 36 (1972) 407–477.
[41] J. Yang, W. Wang, X. Wei, L. Qiu, L. Wang, H. Zhang, L. Song, Peptidoglycan recognition protein of *Chlamys farreri* (CfPGRP-S1) mediates immune defenses against bacterial infection, Dev. Comp. Immunol. 34 (2010) 1300–1307.
[42] A.A. Pal'tsyn, F.G. Kolokol'chikova, A.K. Badikova, N.V. Chervonskaya, I.A. Grishina, The role of agglutination in bacterial infection, Bull. Exp. Biol. Med. 127 (1999) 1–4.
[43] A. Bauer, Ø. Østensvik, M. Florvåg, Ø. Ørmen, L.M. Rørvik, Occurrence of *Vibrio parahaemolyticus, V. cholerae*, and *V. vulnificus* in Norwegian blue mussels (*Mytilus edulis*), Appl. Environ. Microbiol. 72 (2006) 3058–3061.